SSRG International Journal of Mechanical Engineering
ISSN: 2348-8360/ https://doi.org/10.14445/23488360/IJME-V12I2P106

Volume 12 Issue 2, 58-74, February 2025

Original Article

Multi-Objective Optimization of Bead Morphology Using 1.36 Cr-0.5 Mo Steel Metal-Cored Wires for GMAW-Based WAAM

Prerna Shah[1,2], Vyomesh Buch[3], Jay Vora[4]

[1]*Faculty of Engineering and Technology, Parul University, Vadodara, Gujarat, India.*
[2]*Department of Mechanical Engineering, Government Engineering College, Bharuch, Gujarat, India.*
[3]*Parul Institute of Technology, Parul University, Vadodara, Gujarat, India.*
[4]*Department of Mechanical Engineering, School of Technology, Pandit Deendayal Energy University, Gandhinagar, Gujarat, India.*

[1]*Corresponding Author : prerna..shah003@gmail.com*

Received: 08 December 2024 Revised: 09 January 2025 Accepted: 10 February 2025 Published: 25 February 2025

Abstract - *The prime aim of the present investigation was to optimize the process variables to achieve optimum performance of the Gas Metal Arc Welding technique (GMAW) of Wire Arc Additive Manufacturing (WAAM) using Metalloy 80B2 (1.00-1.50% chromium and 0.50% molybdenum steel), a gas-shielded metal-cored wire. The impact of variation in input variables (travel speed, shielding gas composition and voltage) was investigated in terms of Bead Width (BW), Bead Height (BH), and Depth of Penetration (DOP) of bead deposition. The Box Behnken Design of response surface methodology was used to obtain the optimum combination of input parameters for experimentation. The significance and adequacy of correlation developed from the outcomes of experimentation were verified using ANOVA. The travel speed was found to be a more important parameter for DOP and BH, whereas voltage for BW. The main effect and residual plots were studied to identify the most significant influencing independent variable on the response and assess the quality of developed correlations (for DOP, BH, and BW). The Grey Relational Analysis (GRA) was used to find the optimum condition of input variables to achieve the best response. The optimum value of input parameters from GRA was obtained: voltage = 26 V, travel speed = 6 mm/s, and 5% CO_2 in the gas mixture. For the optimum input parameters obtained from GRA, the experimental work was conducted, and an average discrepancy in the result of experimentation was found to be less than 6%. The multilayer structure obtained from experimentation with the optimum parameter was free from disbanding.*

Keywords - *Metal cored wire, Minitab software, Low alloy steel, Wire arc additive manufacturing, Response surface methodology.*

1. Introduction

Over the decades, manufacturing technologies have drastically evolved from conventional manufacturing technology to new technology, such as additive manufacturing. In conventional manufacturing technology, the material is eliminated from the surface of raw material and requires a number of machining operations to prepare the finished product. [1] Whereas in additive manufacturing, the finished products are prepared by laying down and bonding a large number of successive thin layers of raw material. [2] 3-D printing, another name for the additive manufacturing process, is utilized to create complex design structures, large-size objects, unique dimension objects, etc. [3] The benefits of additive manufacturing are such lesser energy consumption, energy efficiency technique, minimum auxiliary equipment required, reduced raw waste material, cost savings, etc. Among the various types of additive manufacturing techniques, direct energy deposition has advantages such as a high rate of deposition, speed of deposition, lower overall cost of manufacturing, the ability to print functionally graded material, the ability to print huge structures, etc., than other methods. The direct energy deposition additive manufacturing techniques of Wire Arc Additive Manufacturing (WAAM) have benefits such as simple handling, a safe environment, reduced material cost, etc. WAAM is classified based on Gas Tungsten Arc Welding (GTAW), Double Electrode GMAW (DE-GMAW), Gas Metal Arc Welding (GMAW), and Cold Metal Transfer (CMT). In GMAW-WAAM, also known as metal inert gas welding, an arc is struck among the base metal workpiece and consumable electrode that provides filler material for welding. GMAW is appropriate for mass production because

of its high deposition rate of 3 to 4 kg/h, high energy efficiency of 84%, high welding speed, high-quality welding with lower spatter, ability to weld thin materials, etc [4-7]. The process parameters such as shield gas composition, wire feed, shielding gas flow rate, wire material, voltage, travel speed of torch, and torch route are crucial parameters for the bead deposition created using GMAW. The wire material used in GMAW has a prominent influence on the product prepared using the weld beads, influencing mechanical properties, surface quality, and dimensional precision. [2, 3] The criteria for the material selection for wire in GMAW rely on the availability of material, cost of material, material properties, manufacturing consideration, fabrication, service and economic requirements.

Henckel et al. [8] built wall structures layer-by-layer with alloy (aluminum-titanium, composition in the range of 10% and 55% aluminum) by varying the feeding rates using GMAW combined with hot-wire feeding. A macroscopic characteristic, the change of the microhardness values of wall structure, and microstructural formation were analyzed. Henckel et al. [9] concluded from the study that nearly 40% of input energy was reduced in the current controlled GMAW-WAAM process by adjusting the distance between the contact tube and workpiece, which improved the geometrical and microstructural features in low-alloyed steel.

Using Response Surface Methodology (RSM), Kumar and Maji [10] developed Box-Behnken Design (BBD) experiments were used to deposit 304L stainless steel in WAAM utilizing a single-bead geometry model. In terms of input parameters such as torch speed, gas flow rate, wire feed rate, and voltage, a correlation between the bead geometry in terms of Bead Width (BW), Bead Height (BH), cross-sectional area, etc., was determined. A genetic algorithm was used to establish the optimal deposition process conditions to decrease void and enhance material yield.

Bharat Kumar and Anand Krishna [11] studied the impact of input parameters of the WAAM process, such as voltage, welding speed, and wire feed speed, on the width of Inconel 825 material bead deposited using metal inert gas welding. For the optimized parameter (voltage = 18 V, welding velocity = 0.55 m/min, and wire feed speed = 4 m/min) using the Taguchi method, the least BW of 3.07 mm length was found. The authors concluded that waviness, discontinuity of surface weld bead, porosity, and weld fractures are lowered by selecting and optimizing the variables.

Baby and Amirthalingam [12] studied the metal transfer characteristic in the GMAW-WAAM process and its impact on microstructural evaluation to recommend an optimal deposition technique. The result indicated that the microstructure of short-circuited pulsed mode deposition formed randomly oriented near equiaxed grains, whereas long and columnar grains were observed using conventional pulsed mode deposition. Pringle et al. [13] found that the most impactful sensors were light and radio frequency for GMAW-based 3-D printing WAAM (with aluminum wire feed) for near-net shape applications, which exhibited a characteristic "good weld" peak frequency and extinction events.

Aldalur et al. [14] studied the three working modes (cold arc, pulsed AC, and pulsed GMAW) to analyze aluminum alloy 5356 in the GMAW-based WAAM technological process. They found the pulsed AC mode better than the other two modes based on evaluating geometrical shape and porosity levels and the finished products.

Zhao et al. [15] developed a mathematical model to simulate fluid flow, geometry morphology, and heat transfer in a GMAW-based WAAM process with Al-5%Mg wire. A maximum velocity of 0.9 m/s was observed when a droplet fell into the molten pool, causing the liquid metal to flow towards the bottom of the molten pool in the middle and forming a depressed region. Further, the deposit profile was compared for the experimental and simulated results.

Mookara et al. [16] attempted to determine the optimal deposition parameter for producing directionally solidified Inconel 625 components by short-circuiting mode of droplet transfer and short-circuiting with pulse mode using CMT GMAW-based WAAM. With improved mechanical and corrosion-resistant properties, a defect-free deposit with desirable microstructure was found for the Inconel 625 components prepared using short-circuiting with pulse mode.

Warsi et al. [17] created a single square bead of ER70S low carbon alloy mild steel wire on the preheated and normal substrate using computer numerically controlled GMAW-based WAAM to analyze the bead humping and control of BH dimensional stability phenomenon. An improvement in hardness, lower wear, reduced humping, and higher dimensional stability was found for the bead deposited on the preheated substrate using WAAM than the conventional method.

Vishal Kumar et al. [18] carried out a study to obtain the optimized process variables for the deposition of single-layer weld bead of copper-coated mild steel ER70S-6 metallic wire created using the GMAW-WAAM process. A maximum height and minimum width of single-layer bead were obtained for the optimal process parameters such as travel speed = 95 mm/min shielding gas flowrate = 21 L/min. Open circuit voltage = 16 V.

The author previously examined the travel speed, impact of voltage, and wire feed speed on the BH and BW for multiple beads of low alloy steel multiple layers prepared using the GMAW-WAAM process. The regression equations

were developed among the input and output parameters, and robustness and adequacy were examined using Analysis of Variance (ANOVA). For the optimized input parameter, BW = 4.73 mm and BH = 7.81 mm were obtained, and the structure was found free of disbonding. The author previously examined the effect of travel speed, wire feed speed, and voltage on BH and BW for a multilayer structure built with SS 316L metallic wire using the GMAW-WAAM process.

The multivariable regression equations were developed between the response and design variables, and feasibility was analyzed using ANOVA. Wire feed speed was found to be the highest contributing factor affecting the BW and BH. For the optimized input parameter (voltage = 19 V, wire feed speed = 5.50 m/min, and travel speed = 141 mm/min), BH = 7.81 mm and BW = 5.01 mm were observed for the multilayer structures, and seamless fusion and the structure found free of disbonding.

The literature indicates that majorly the research work on WAAM process was conducted using titanium alloy such as Ti6Al4V [19], β-titanium alloy [20], etc., aluminium alloy such as TiC/AA7075 [21], AlMg5Mn [22], etc., and low carbon steel like 316L stainless steel, 1.25Cr-1.0Mo steel, etc. as wire material. Using a combination of materials and alloys can enhance the properties of single and multilayer bead structures. However, very little research work on the WAAM process was observed in the literature with the use of low-alloy steel. Further, the literature indicates the influence of process/ input parameters such as voltage, travel speed, and wire feed speed on response parameters was investigated for the GMAW-WAAM process, but the impact of the shielding gas composition was not observed.

To fulfil the research gap, Metalloy 80B2 wire (1.00 - 1.50% Chromium, 0.50% Molybdenum), a low-alloy steel gas-shield metal-cored wire, was employed to create the bead deposition using GMAW-based WAAM process in the present investigation. An impact of process/input parameters such as voltage (22 to 26 V), travel speed (1 to 6 mm/s), and shielding gas composition (CO_2 - 1%, 5%, and 9% and Argon - 99%. 95%, and 91%) was investigated on response parameters such as Depth of Penetration (DOP), BH and BW for the bead deposition created using GMAW-WAAM. The BBD was used to find the optimum combination of input variables (voltage, travel speed, % of CO_2 into gas mixture) using Minitab v21 software for the experimental work.

The correlations for the response parameters were developed as a function of input parameters. An ANOVA analysis was carried out to verify the significance of developed correlations, and fit statistics were conducted to examine the performance of forecasting correlations. The main effect plot and residual plots were studied to identify the most significant influencing independent variable on the response and to assess the quality of developed correlations (for DOP, BH, and BW). The Grey Relational Analysis (GRA) was used to determine the optimal input parameters (voltage, travel speed, and percentage of CO_2 in gas mixture) for the best response. The validation of outcomes of GRA for optimized input parameters was compared with the outcomes of experimentation for the optimized parameter.

The paper is structured as follows: Section 2 depicts the experimental setup, Section 3 depivts the methodology, and Section 4 depicts design of experiments using BBDs. Section 5 depicts the results and discussion, which includes results of experimentation, development of correlation, ANOVA analysis, main effect plot, residuals plot for the response parameters, GRA for optimum input parameter, and experimentation for the optimized input parameters. Section 6 presents the conclusion of the present research work.

2. Experimental Setup, Methodology, and Design of Experiment

2.1. Experimental Setup

Figure 1(a) and (b) depict the 3-D model and experimental setup of the GMAW-based WAAM process. The experiment apparatus consisted of a welding torch, working table, shielding gas cylinder, wire feeder, computer interface, automated nozzle controller, power source, and control unit. In the present investigation, shielding gas utilized for bead deposition comprised a mixture of varying percentages of Argon (99%. 95%, and 91%) and CO_2 (1%, 5%, and 9%). For specific bead deposition, the program code was developed and executed via a computer interface. The navigation of the automated nozzle controller along the X, Y, and Z coordinates was governed by a program code developed via a computer interface.

Before the commencement of each program run, shielding gas was supplied into the setup to prevent contact between the deposited material and air gases. The versatile welding torch, able to move in a specific direction as per requirement in experimental work, was utilized for the bead deposition on the base metal, which was clamped from all sides on the working table. In the present investigation, Metalloy 80B2 (chrome-moly steels), a gas-shielded metal-cored wire, was employed for bead deposition in single or multiple passes. Metal-cored wire was chosen because of its higher penetration and deposition rate than solid wire and flux-coated wire. Table 1 depicts the chemical composition of metal-cored wire (Metalloy 80B2). A diameter Metalloy 80B2 wire was 1.2 mm and procured from Hobart Brothers (TRI-MARK).

3. Response Surface Methodology

For the optimum performance of a process or system, the operating parameters of the process or system need to be optimized or need a proper design of the experiment, which reduces the experimental iteration, time duration, and the cost

of operating to quest for the optimum performance. The optimization technique is a powerful tool for obtaining the optimum parameter and optimum set of operating conditions for the experimentation. An optimization technique or methodology utilized for designing the experiments or to obtain the optimum set of conditions of parameters must be cost-effective.

[23] RSM is a convenient and powerful statistical tool that helps the researcher to systematically design a set of experiments for the optimization of operating parameters. [24] RSM uses the factorial technique and ANOVA to model the response parameter as a function of multiple input parameters. RSM assist in finding the best setting for the factorial variable to achieve a desired maximum or minimum response. The utilization of RSM for the optimization of parameters has benefits such as being cost-effective and efficient, requiring fewer experiments, identifying the optimal conditions, determining the interaction among the variables, simplifying the process of fitting, providing the visual representation, etc. Among the types of RSM, BBDs were used for optimization in the present investigation.

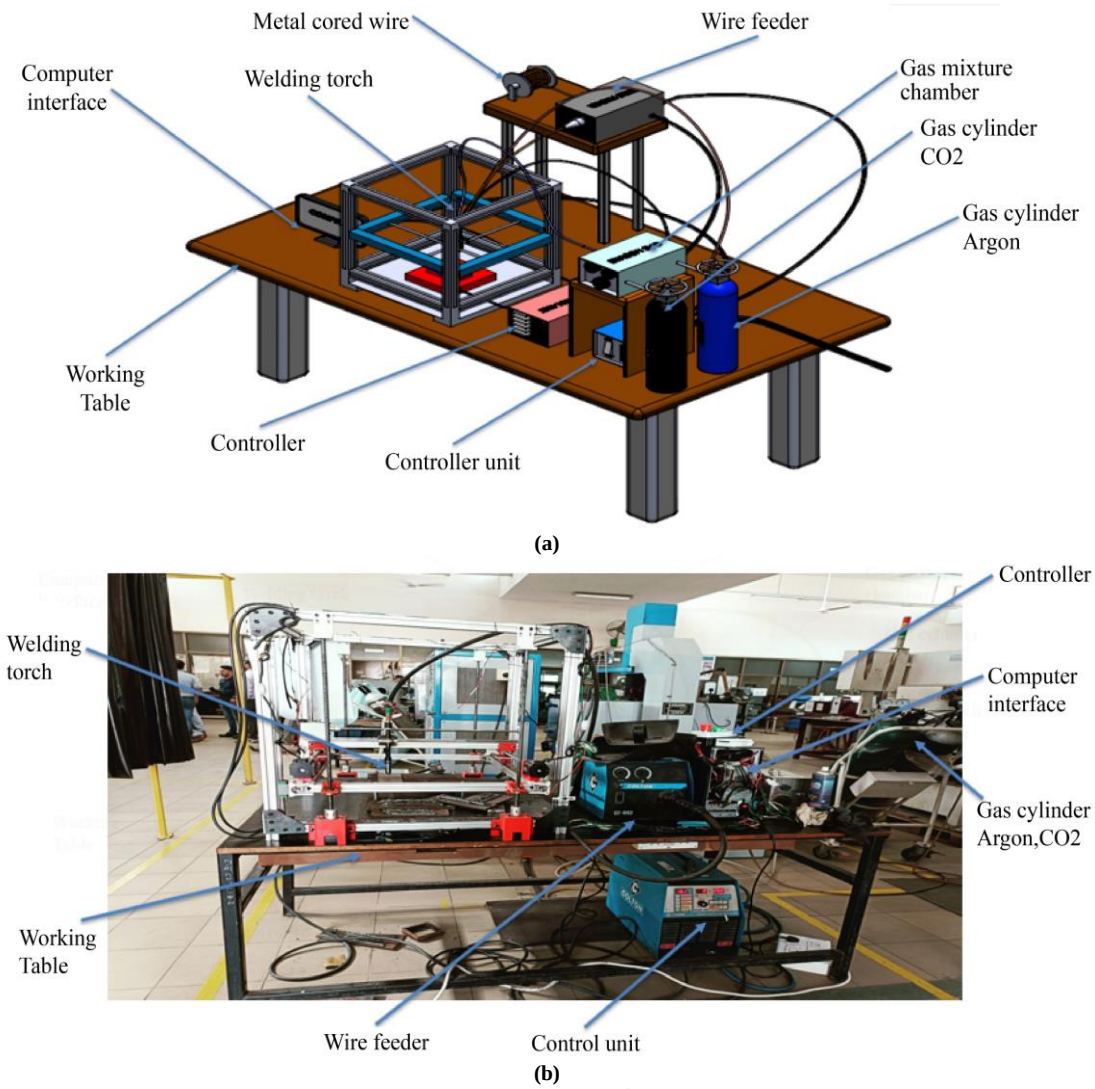

Fig. 1 (a) 3-D model, and (b) experimental setup of GMAW-based WAAM process.

Table 1. Composition of Metalloy 80B2 metal-cored wire

Detail	Mo	Cr	C	Si	Mn	Fe
0.50% Molybdenum, 1.00 - 1.50% Chromium (Metal - cored wire)	0.5	1.36	0.06	0.29	0.82	Balance

4. Design of Experiment Using Box-Behnken Designs

The BBDs, the experimental designs for RSM, are independent quadratic designs that can be used to fit a quadratic model and generate higher-order response surfaces with few runs. The BBDs are the type of rotatable or nearly rotatable second-order designs based on three-level incomplete factorial designs that require a minimum of three factors. In BBDs, treatment combinations are at the midpoints of the edges of the process and at the center. The voltage (V), travel speed (S), and percentage of CO_2 in gas mixture ratio are chosen as input parameters for optimization, whereas Depth of Penetration (DOP), BH, and BW are chosen as response parameters to study the impact of input parameters. The variation in input parameters for the study was chosen: for voltage (V), in the range of 22 to 26 V with the step size of 2 V; for travel speed, in the range of 6 to 10 mm/s with the step size of 2 mm/s; for percentage of CO_2 in gas mixture ratio, in the range 1 to 9% with the step size of 4%. The value of other parameters such as arc length, length of bead, and gas flow rate was chosen as 3 mm, 150 mm each, and 15 L/min based on a literature survey and the machining ability of the system. Figure 2 depicts the image of the application of BBD to examine the influence of input parameters on the outcome/response parameters. The Minitab v21 software was used for the optimization process. The BBDs predicted 15 runs for experimentation to achieve optimal process or system performance. Table 2 depicts the combination of input variables for each run or optimal performance.

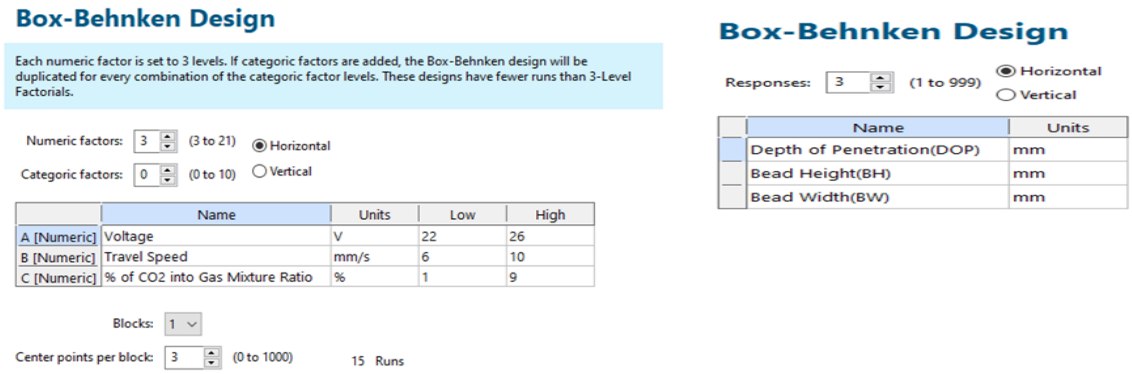

Fig. 2 Design of experiment using BBD

Table 2. Value of input parameter for various run

Run Order	Standard Order	Input Parameter or Factor -1	Input Parameter or Factor -2	Input Parameter or Factor -3
		Voltage (V)	Travel Speed (mm/s)	% of CO_2 in the Gas Mixture Ratio
1	13	24	8	5
2	9	24	6	1
3	5	22	8	1
4	12	24	10	9
5	2	26	6	5
6	6	26	8	1
7	8	26	8	9
8	14	24	8	5
9	3	22	10	5
10	11	24	6	9
11	10	24	10	1
12	1	22	6	5
13	4	26	10	5
14	15	24	8	5
15	7	22	8	9

5. Result and Discussion

5.1. Result of Experimentation

A 15 experimental run was performed on the experimental setup described in subsection 2.1 with the combinations of input parameters predicted using the BBDs technique (subsection 2.3) for the optimum performance. The single-layered deposition of metal-cored wire Metalloy 80B2 on the base plate for the 15 experimental run is shown in Figure 3. Single-layer deposition was cut into cross-sections or pieces to measure the response parameters such as DOP, BH, and BW. The optical microscopy technique was employed for the measurement of response parameters such as DOP, BH, and BW. Each response parameter was measured three times to avoid measurement error, and the average value of three measured values of the response parameter for each experimental run is depicted in Table 3. The measured value of experimentation results was observed in the range of ± 5%.

5.2. Correlation for DOP, BH, and BW

To establish the correlation among the input parameter (voltage, travel speed, and % of CO_2 in gas mixture) and response parameter (DOP, BH, and BW), the response surface model (using Minitab v21 software) was developed using RSM and is presented as Equations (1), (2), and (3), respectively. The correlation for DOP indicates the inclusion of linear, mixture, and quadratic terms of the input variable, indicating the non-linear relation among the input and response parameters. Meanwhile, the correlation for BH and BW indicates a linear relationship with input variables. The established correlations help to predict the response parameter before executing the experimentation that can be utilize to optimize the performance of the process for the researcher working in the field of the research paper. This will save time and that saves the time and economy for the resources (monetary, physical and infrastructural, etc.) of the researchers and industrial adaptions as well.

$$DOP = 22.63 - 0.9350 \times X_1 + 1.809 \times X_2 + 0.1109 \times X_3 - 0.0881 \times X_2^2 \quad (1)$$

$$BH = -10.26 + 0.327 \times X_1 + 1.068 \times X_2 + 1.562 \times X_3 - 0.0466 \times X_1 \times X_3 - 0.0494 \times X_2 \times X_3 \quad (2)$$

$$BW = 7.35 - 0.581 \times X_1 - 0.07637 \times X_2 - 0.0832 \times X_3 + 0.01418 \times X_1^2 + 0.002843 \times X_3^2 + 0.00908 \times X_2 \times X_3 \quad (3)$$

Where, X_1, X_2, and X_3 indicates voltage (V), travel speed (mm/s), and % of CO_2 into gas mixture (%).

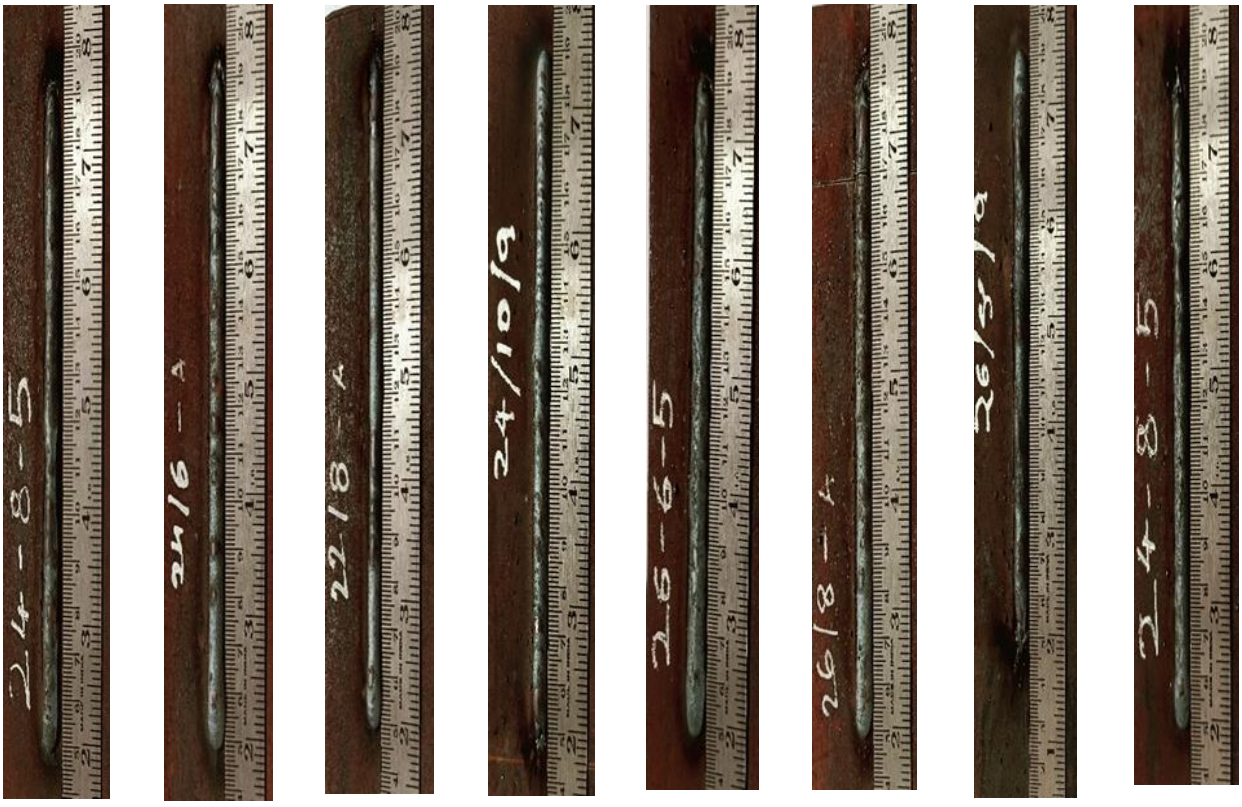

Run-1 **Run-2** **Run-3** **Run-4** **Run-5** **Run-6** **Run-7** **Run-8**

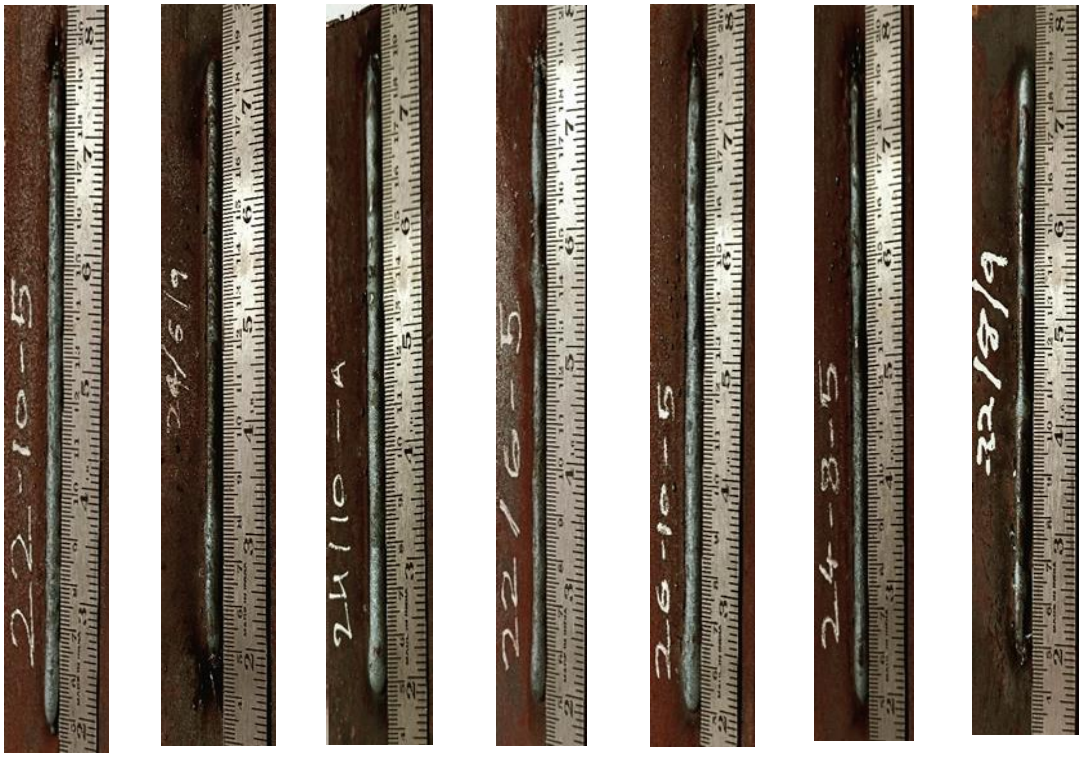

Run-9 Run-10 Run-11 Run-12 Run-13 Run-14 Run-15

Fig. 3 Single-layered deposition of metal-cored wire Metalloy 80B2 on the base plate

Table 3. Output of experimentations

Run Order	Standard Order	Input-1	Input-2	Input-3	Output-1	Output-2	Output-3
		Voltage (V)	Travel Speed (mm/s)	% of CO_2 into the Gas Mixture	DOP (mm)	BH (mm)	BW (mm)
1	13	24	8	5	0.9777	6.61	9.26
2	9	24	6	1	1.0817	4.11	8.11
3	5	22	8	1	0.8129	5.23	10.74
4	12	24	10	9	1.1294	7.81	10.67
5	2	26	6	5	1.3198	4.93	6.97
6	6	26	8	1	1.2156	6.72	7.36
7	8	26	8	9	1.3018	6.72	8.21
8	14	24	8	5	0.9668	6.49	9.46
9	3	22	10	5	0.7674	7.84	11.81
10	11	24	6	9	1.1034	4.95	8.49
11	10	24	10	1	0.8172	8.55	10.02
12	1	22	6	5	0.8971	4.95	10.14
13	4	26	10	5	1.1923	7.88	9.46
14	15	24	8	5	0.9603	6.27	7.6
15	7	22	8	9	0.9625	6.72	11.81

5.3. ANOVA for DOP, BH, and BW

The ANOVA is utilized to predict the F-value and p-value for the established correlation in subsection 3.2. The results obtained from the ANOVA are depicted in Table 4 for DOP, Table 5 for BH, and Table 6 for BW. The sum of squares is a statistical term used in regression analysis to study the data point dispersion. A lower sum of squares indicates lower variability, whereas a higher indicates high variability from the mean.

The F-value indicates whether the null hypothesis should be accepted or rejected. The high F-value indicates the model

is significant. The p-value measures the probability of getting the observed outcomes, presuming the null hypothesis is true. The p-value lesser than 0.05 represents that the model is statistically significant.

The p-value and F-value for the DOP obtained from ANOVA is 0.000 and 114.10 indicating the model/correlation of DOP is significant. From the result of ANOVA for DOP, travel speed (represented by parameter X_2) is more important than the other input parameters in the model/correlation of DOP. The F-value and p-value for the BH obtained from ANOVA are 48.67 and 0.000, indicating the model/correlation of BH is significant. From the result of ANOVA for BH, travel speed (represented by parameter X_2) is found to be more important than the other input parameters in the model/correlation of BH.

The F-value and p-value for the BW obtained from ANOVA is 64.01 and 0.000, indicating the model/correlation of BW is significant. From the result of ANOVA for BW, voltage (represented by parameter X_1) is found more important than the other input parameters in the model/correlation of BW.

Table 4. ANOVA results for DOP

Value of	Degree of Freedom	Adjusted Sum of Square	Adjusted Mean Square	F-Value	P-Value	Conclusion
Correlation	6	0.426590	0.071098	114.40	0.000	*
Linear Term in the Model	3	0.054714	0.018238	29.35	0.000	*
X_1 - Voltage (V)	1	0.008705	0.008705	14.01	0.006	*
X_2 -Travel Speed (mm/s)	1	0.045247	0.045247	72.81	0.000	*
X_3 - % of CO_2 in gas mixture	1	0.019093	0.019093	30.72	0.001	*
Square Term in the Model	2	0.018354	0.009177	14.77	0.002	*
$X_1 \times X_1$	1	0.011945	0.011945	19.22	0.002	*
$X_3 \times X_3$	1	0.007684	0.007684	12.36	0.008	*
2-way Interaction in Model	1	0.021098	0.021098	33.95	0.000	*
$X_2 \times X_3$	1	0.021098	0.021098	33.95	0.000	*
Error	8	0.004972	0.000621			
Lack-of-Fit	6	0.004817	0.000803	10.39	0.090	#
Pure Error	2	0.000155	0.000077			-
Total	14	0.431562				-
"#" indicates non-significance and "*" indicates significance. **Model Summary:** R^2 = 98.85%; Adjusted R^2 = 97.98%; Predicted R^2 = 94.96%.						

The lack of fit indicates the variation of the designed point about predicated value. It should be insignificant for the model to fit well in experimental data, indicating the lower value of lack of fit is preferable.

The F-value of lack of fit obtained from ANOVA for DOP, BH, and BW was 10.39, 3.87, and 5.31, and the p-value of lack of fit obtained from ANOVA for the DOP, BH, and BW was 0.090, 0.221, and 0.168, indicating not significate or predicated model/correlations are adequate.

Fit statistics indicate statistical values utilized to examine the performance of the forecasting model by comparing actual data to the predictions. The predicted R^2 represent how the regression model/correlation predicts/accurately responds to new observations. The adjusted R^2 accounts/penalizes the variables that are not significant in the regression model/correlation. In other words, adjusted R^2 provides an accurate model/correlation that fits the current data, whereas predicted R^2 determines how likely that model/correlation is accurate for future data.

The adjusted R^2 and predicted R^2 values for DOP were 97.98% and 94.96%, indicating that the model/correlation is accurate for predicting response parameters as the difference among adjusted R^2 and predicted R^2 is less than 0.2.

The adjusted R^2 and predicted R^2 values for BH were 94.45% and 85.85%, indicating that the model/correlation accurately predicts response parameters. The adjusted R^2 and predicted R^2 values for BW were 94.74% and 90.61%, indicating that the model/correlation accurately predicts response parameters.

Table 5. ANOVA results for BH

Value of	Degree of freedom	Adjusted sum of square	Adjusted mean square	F-Value	P-Value	Conclusion
Correlation	5	23.3626	4.67252	48.67	0.000	*
Linear term	3	11.0666	3.68888	38.43	0.000	*
X_1 - Voltage (V)	1	0.8305	0.83046	8.65	0.016	*
X_2 -Travel Speed (mm/s)	1	8.8505	8.85055	92.20	0.000	*
X_3 - % of CO_2 in gas mixture	1	0.9731	0.97313	10.14	0.011	*
2-way interaction term	2	1.1791	0.58956	6.14	0.021	*
$X_1 \times X_3$	1	0.5550	0.55502	5.78	0.040	*
$X_2 \times X_3$	1	0.6241	0.62410	6.50	0.031	*
Error	9	0.8640	0.09600			
Lack-of-Fit	7	0.8045	0.11493	3.87	0.221	#
Pure Error	2	0.0595	0.02973			
Total	14	24.2266				
"#" indicates non-significance and "*" indicates significance. **Model Summary:** R^2 = 96.43%; Adjusted R^2 = 94.45%; Predicted R^2 = 85.85%.						

Table 5. ANOVA results for BW

Value of	Degree of Freedom	Adjusted Sum of Square	Adjusted Mean Square	F-Value	P-Value	Conclusion
Correlation	5	23.3626	4.67252	48.67	0.000	*
Linear term	3	11.0666	3.68888	38.43	0.000	*
X_1 - Voltage (V)	1	0.8305	0.83046	8.65	0.016	*
X_2 -Travel Speed (mm/s)	1	8.8505	8.85055	92.20	0.000	*
X_3 - % of CO_2 in gas mixture	1	0.9731	0.97313	10.14	0.011	*
2-way interaction term	2	1.1791	0.58956	6.14	0.021	*
$X_1 \times X_3$	1	0.5550	0.55502	5.78	0.040	*
$X_2 \times X_3$	1	0.6241	0.62410	6.50	0.031	*
Error	9	0.8640	0.09600			
Lack-of-Fit	7	0.8045	0.11493	3.87	0.221	#
Pure Error	2	0.0595	0.02973			
Total	14	24.2266				
"#" indicates non-significance and "*" indicates significance. **Model Summary:** R^2 = 96.43%; Adjusted R^2 = 94.45%; Predicted R^2 = 85.85%.						

5.4. Main Effect Plot for DOP, BH and BW

The main effect plot is a graphical tool utilized to identify the most significant influencing independent variable or a factor on the response or dependent variable. The main effect plot allows us to isolate and evaluate the impact of individual input variables on the dependent variable of response. By examining the slope and direction of the lines on the plot, the driving or prioritized independent variable or factor that drives the process can be determined.

Figure 4 presents the main effect plot to identify the impact of voltage, travel speed and % of CO_2 in gas mixture on DOP. With the rise from 22 V to 26 V in voltage, an increasing trend has been observed for DOP. The reason was that an increase in voltage caused a higher arc length, which resulted in the spreading of molten droplets and higher material deposition. With the rise in travel speed from 6 mm/s to 10 mm/s, a decreasing trend has been observed for DOP. The reason was an increase in the travel speed of the torch; less material was being deposited due to less time available for the material deposition. With the rise in % of CO_2 in the gas mixture from 1% to 9%, an increasing trend has been observed for DOP. The reason was: a rise in % of CO_2 in the gas mixture, causing an increase in carbon content resulted in higher weld penetration. A rate of increase in slope for voltage has been observed higher than the rate of increase in slope for % of CO_2 in the gas mixture and the rate of decrease in slope for travel speed, indicating the voltage is a crucial parameter for the DOP.

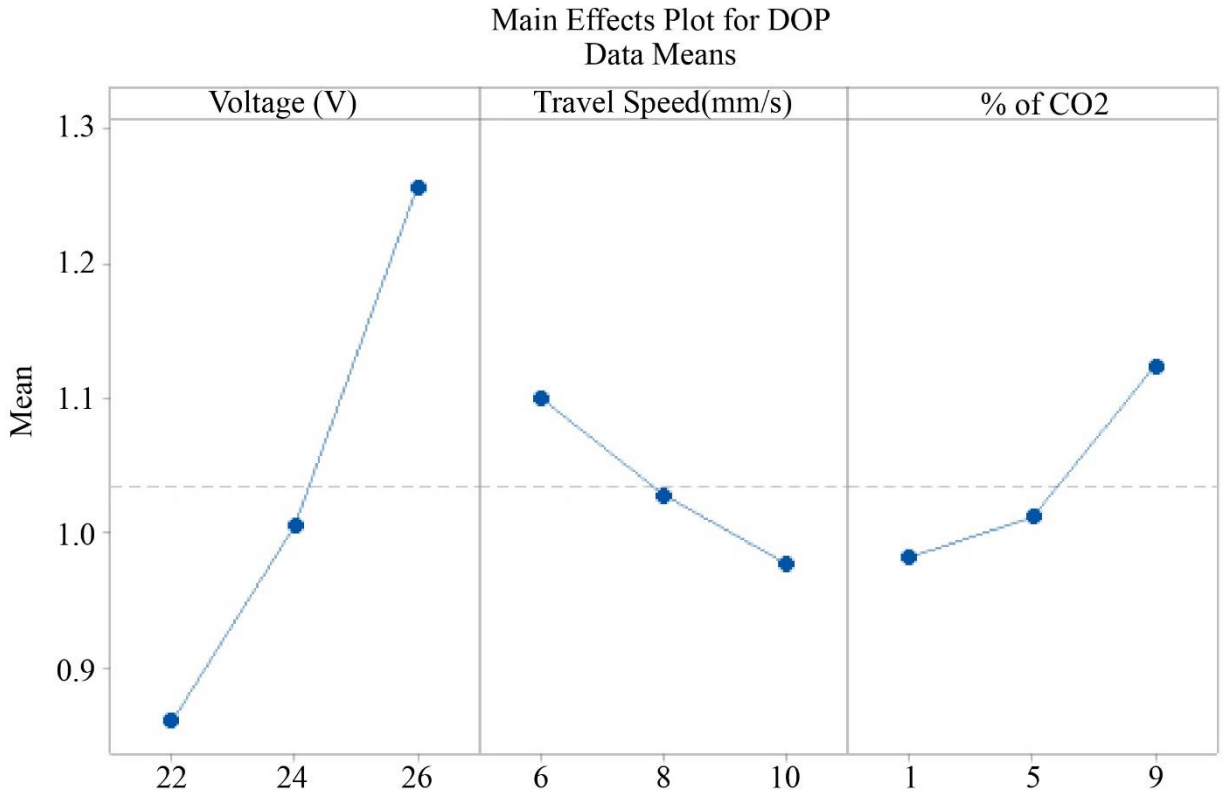

Fig. 2 Main effects plot for DOP

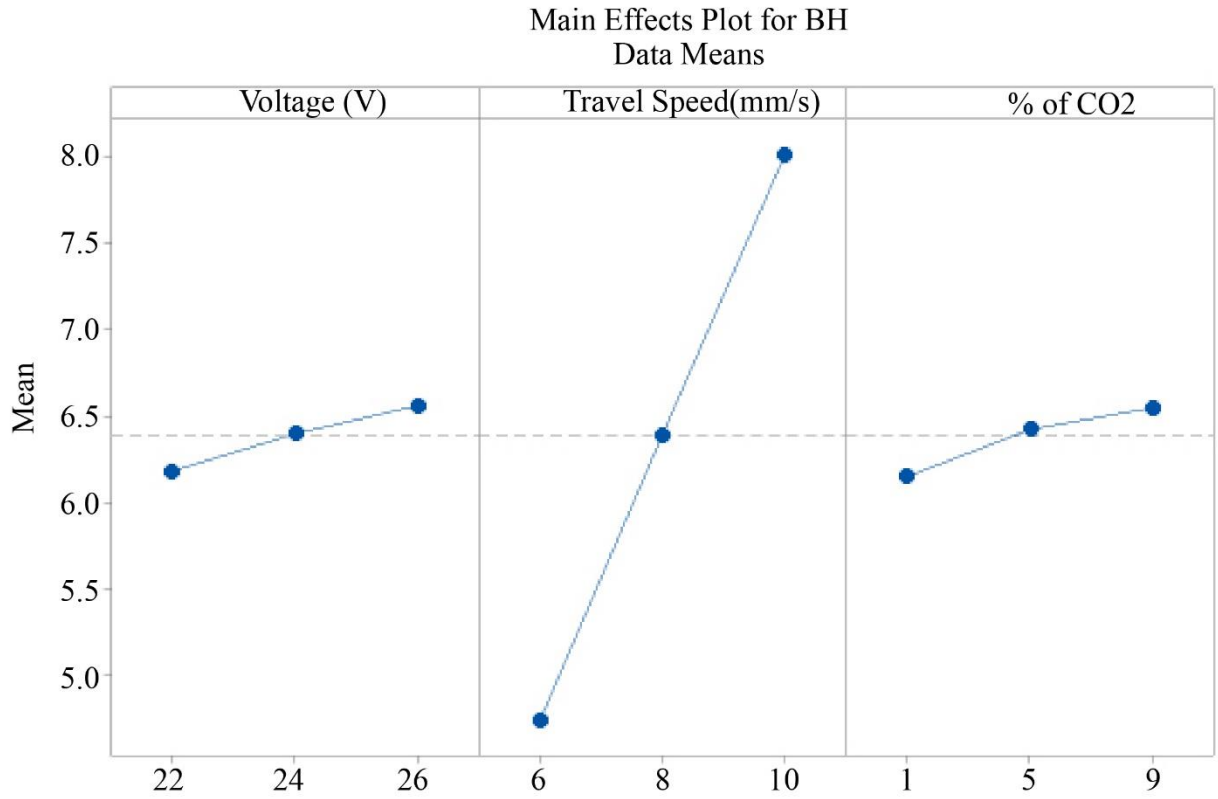

Fig. 3 Main effects plot for BH

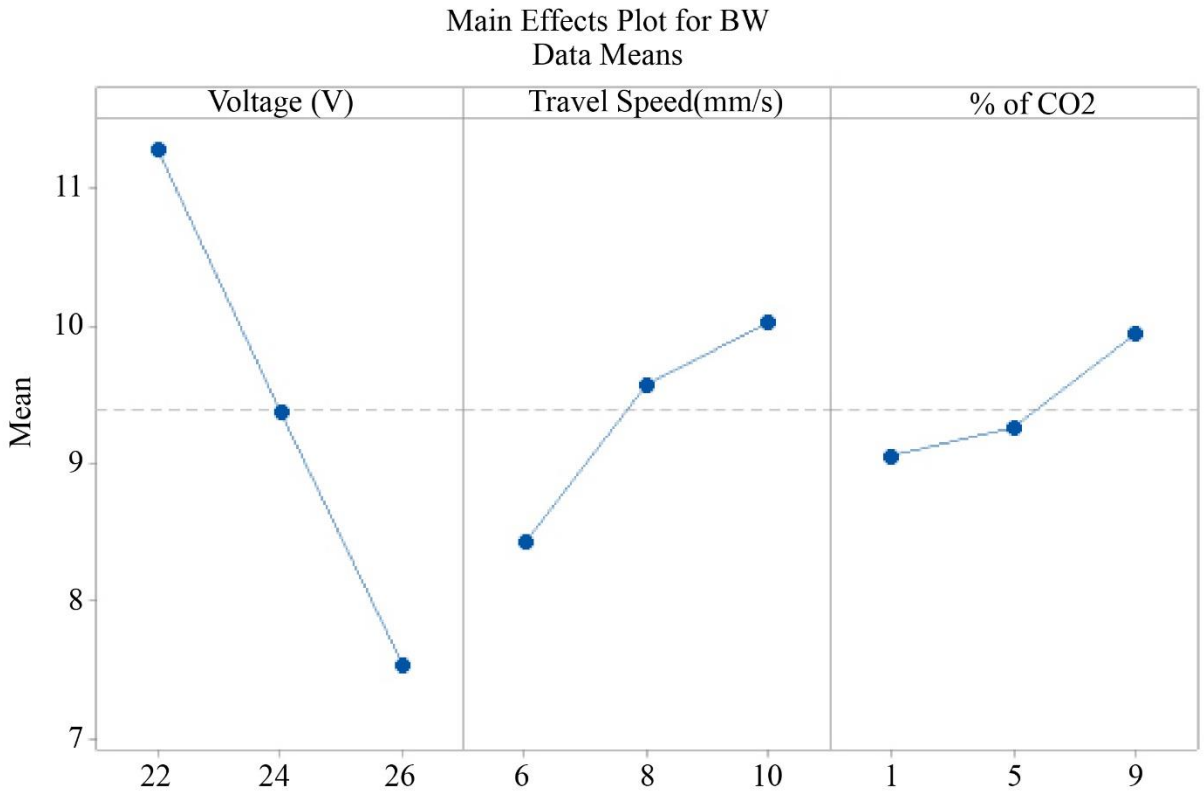

Fig. 4 Main effects plot for BW

The higher the value of the mean for various parameters, the higher the DOP achieved. The higher value for DOP can be obtained for 26 V voltage, travel speed of 6 mm/s, and 9% of CO_2 in the gas mixture.

Figure 5 presents the main effect plot to identify the impact of voltage, travel speed and % of CO_2 in gas mixture on BH. With the rise from 22 V to 26 V in voltage, an increasing trend has been observed for BH. The reason was that an increase in voltage caused a higher arc length, which resulted in the spreading of molten droplets and higher material deposition. With the rise in travel speed from 6 mm/s to 10 mm/s, an increasing trend has been observed for BH. The reason was an increase in the travel speed of the torch; less material was being deposited due to less time available for the material deposition. With the rise in % of CO_2 in the gas mixture from 1% to 9%, an increasing trend has been observed for BH. The reason was a rise in % of CO_2 in the gas mixture, causing an increase in carbon content that prevented air from entering and contaminating the material. A rate of increase in slope for travel speed has been observed to be higher than the rate of increase in slope for % of CO_2 in the gas mixture and the rate of increase in slope for voltage, indicating that travel speed is a crucial parameter for BH. The higher value of the mean for various parameters indicates higher BH achieved. The higher value for BH can be obtained for 10 mm/s travel speed, 26 V voltage, and 9% of CO_2 in the gas mixture.

Figure 6 presents the main effect plot to identify the impact of voltage, travel speed and % of CO_2 in gas mixture on BW. With the rise from 22 V to 26 V in voltage, a decreasing trend has been observed for BW. The reason was that an increase in voltage caused a higher arc length, which resulted in the spreading of molten droplets and higher deposition of material, which resulted in an increase in BW. With the rise in travel speed from 6 mm/s to 10 mm/s, an increasing trend has been observed for BW. The reason was an increase in the travel speed of the torch; less material was being deposited due to less time available for the material deposition. With the rise in % of CO_2 in the gas mixture from 1% to 9%, an increasing trend has been observed for BW. The reason was a rise in % of CO_2 in a gas mixture, causing an increase in carbon content that prevented air from entering and contaminating the material. A rate of decrease in slope for travel speed has been observed higher than the rate of increase in slope for % of CO_2 in the gas mixture and rate of increase in slope for traveling speed, indicating the voltage is a crucial parameter for the BW. The lower mean value for various parameters indicates a higher BW achieved. The higher value for BW can be obtained for 26 V voltage, travel speed of 6 mm/s, and 1% of CO_2 in the gas mixture.

5.5. Residuals Plot for DOP, BH, and BW

Residual indicates the difference between the variable's actual value and predicted value (from the correlation or model) at a given point. Residual plots are utilized to assess

the quality of the developed correlation or model and improve the developed correlation or model for the dependent variable. The residual versus fit plot, normal probability plot of residuals, residual versus order plot, and histogram of the residual plot for the DOP, BH, and BW were presented and studied in the present investigation. The normal probability plot of residuals is a graphical technique that shows the sample percentiles of residuals on the y-axis and theoretical percentiles of normal distribution on the x-axis. It is also used to assess whether the dataset follows the normal distribution or not. If the plot is approximately linear or straight line, indicating error terms are normally distributed. The stronger evidence of normality was depicted when the data points were closer to a straight line. The residual versus fit plot is the scatter plot of the fitted value (estimated response of correlation or model) on the x-axis and the residual on the y-axis. It is utilized to detect non-linearity, unequal error variance and outliers. The residuals are more or less randomly distributed around the zero line, indicating that the linear regression model is suitable for data sets. The histogram of the residual plot shows the distribution of residual observation, which is used to determine whether the data is skewed or whether outliers exist in the data and to check whether the distribution of variance is normal or not. The normality assumption is likely to be true when residuals are evenly distributed around zero in a symmetric bell-shaped histogram. The residual versus order plot is a scatter plot that indicates the order in which data was collected on the x-axis and residuals on the y-axis and used to identify whether residuals are independent of one another or not. The residuals are independent of one another when residuals on residual versus order plots fall randomly around the center line. Figures 7, 8 and 9 present the residual versus fit plot, normal probability plot of residuals, residual versus order plot, and histogram of residuals for DOP, BH, and BW. In the normal probability plot of residuals for DOP, BH, and BW, error terms are closer to the straight line, indicating that error terms are normally distributed. In the residual versus fit plot for DOP, BH, and BW, residuals are randomly distributed around the zero line, indicating that the regression model is suitable for data sets. In the histogram of the residual plot for DOP, BH, and BW, a symmetric bell shape was not observed around zero, indicating a skewed distribution. In the residual versus order plot for DOP, BH, and BW, residuals fall randomly around the center line, indicating that residuals are independent.

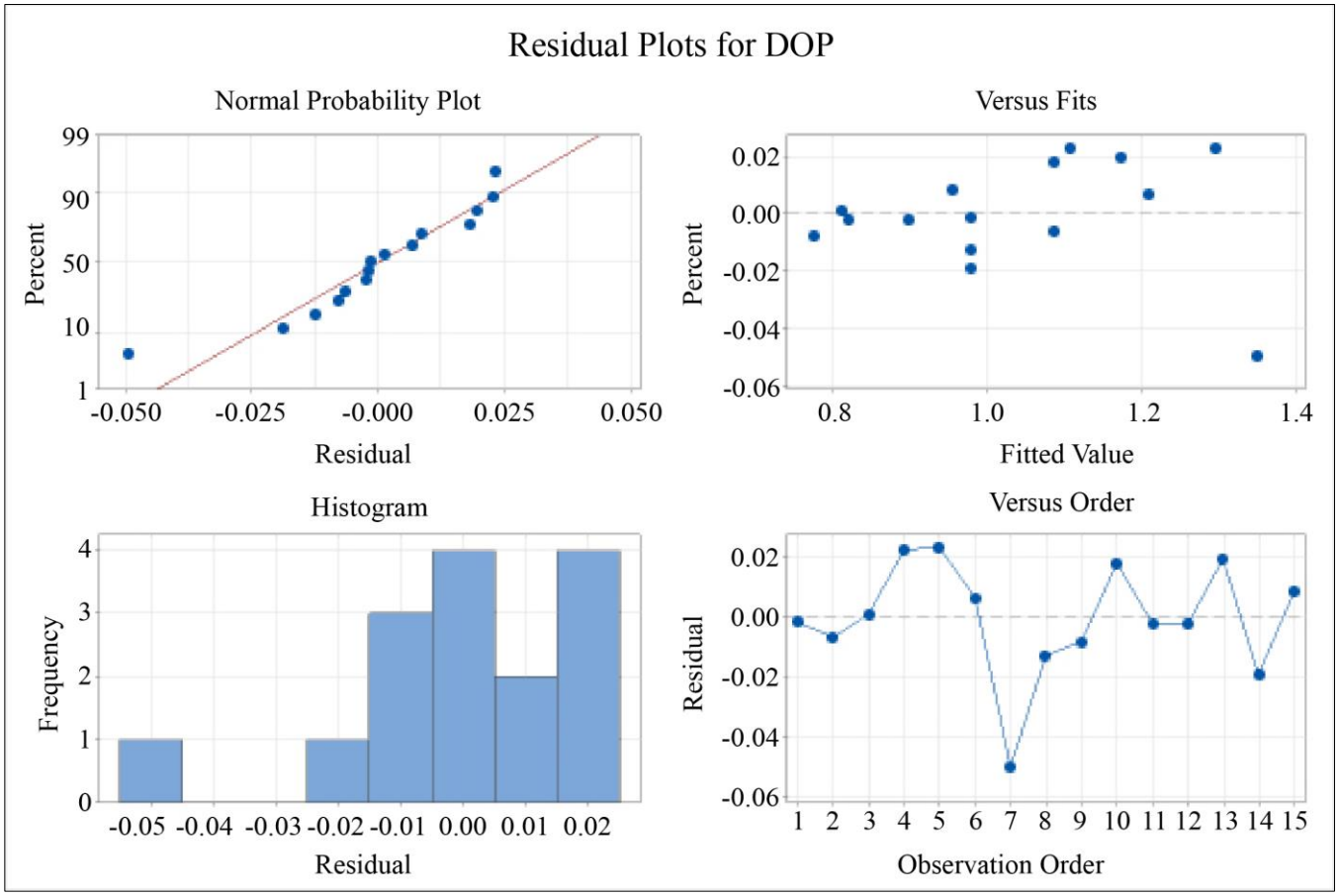

Fig. 5 Residual plot - DOP

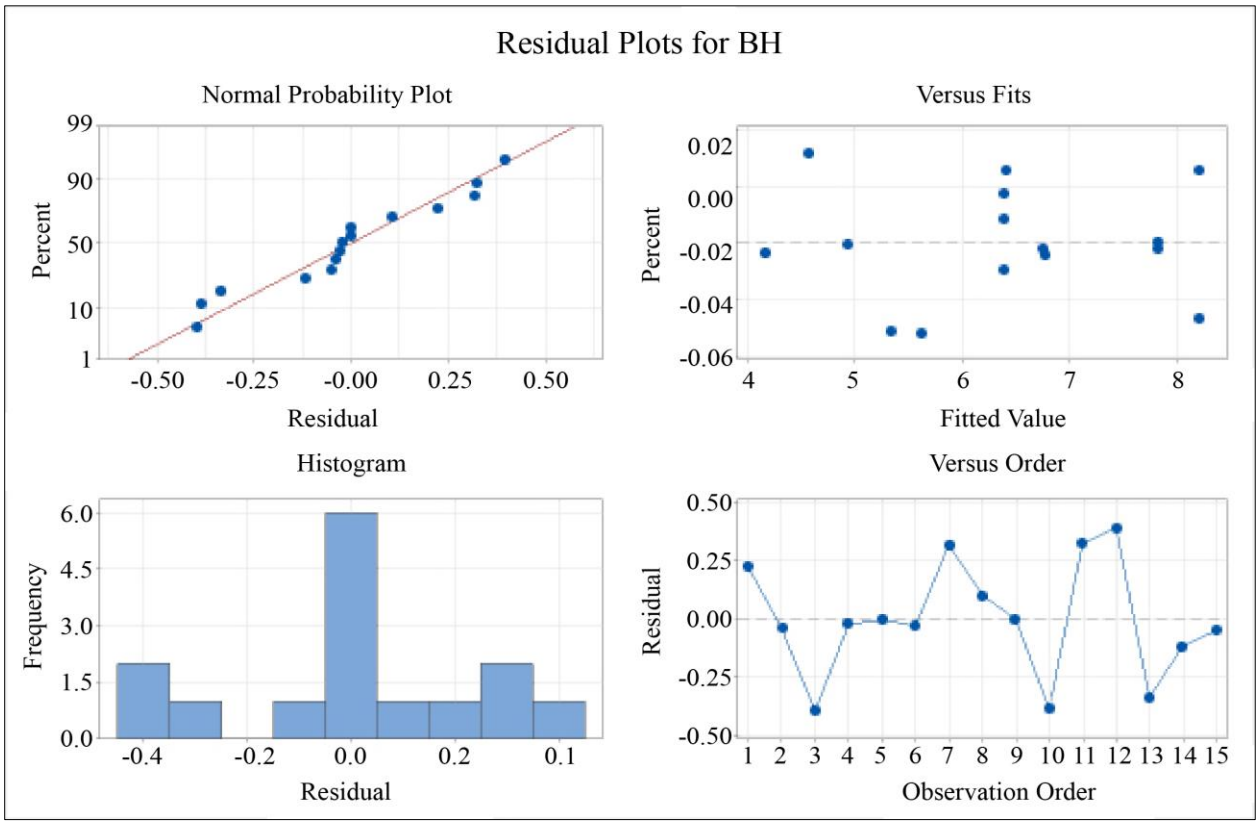

Fig. 6 Residual plot - BH

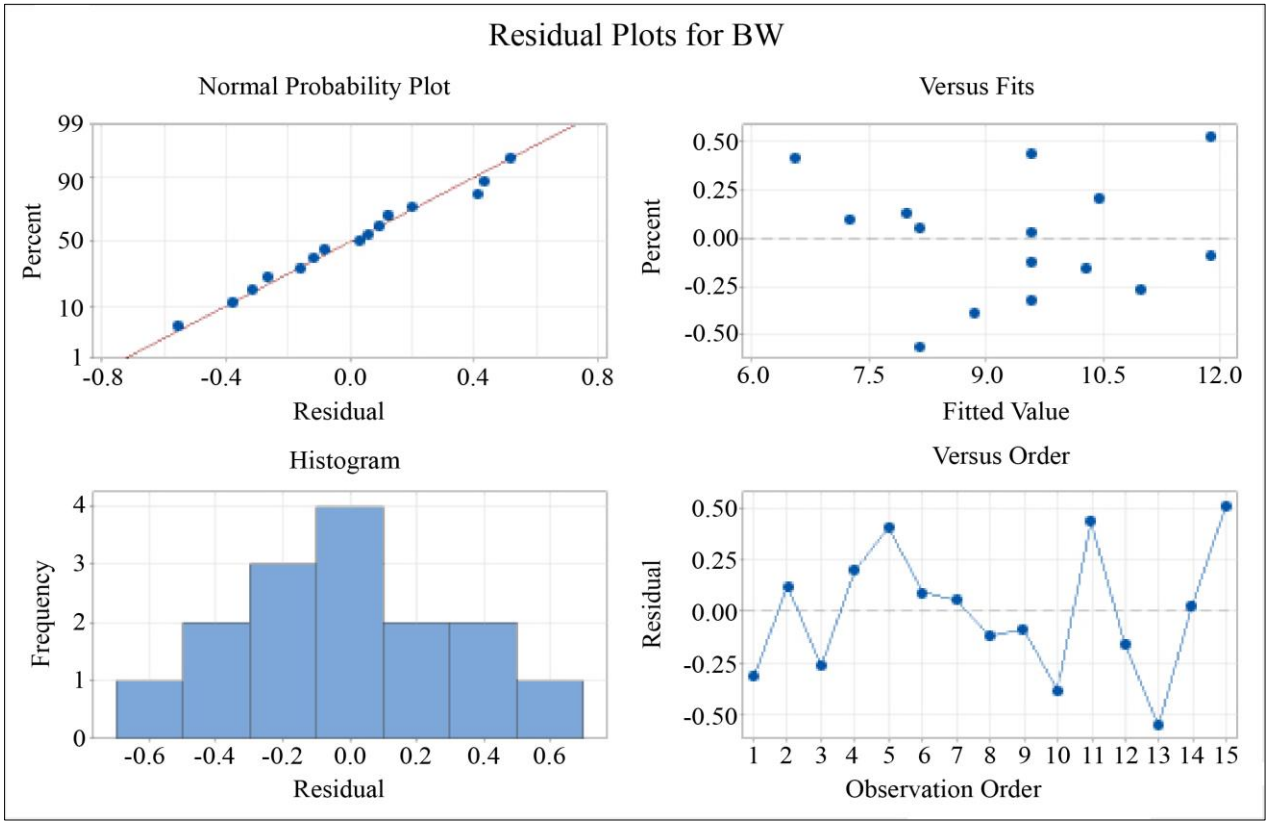

Fig. 7 Residual plot - BW

5.6. Optimization by Grey Relational Analysis

Table 6. Normalization and evaluation of Δoi (k) for the responses

Run order	Normalization			Evaluation of Δoi (k) for each of the responses		
	DOP	BH	BW	DOP	BH	BW
	(larger the better)	(larger the better)	(smaller, the better)	(larger the better)	(larger the better)	(smaller, the better)
1	0.38070239	0.563063063	0.579044118	0.61929761	0.436936937	0.420955882
2	0.56897176	0	0.790441176	0.43102824	1	0.209558824
3	0.082367849	0.252252252	0.306985294	0.917632151	0.747747748	0.693014706
4	0.65532223	0.833333333	0.319852941	0.34467777	0.166666667	0.680147059
5	1	0.184684685	1	0	0.815315315	0
6	0.811368573	0.587837838	0.928308824	0.188631427	0.412162162	0.071691176
7	0.967414917	0.587837838	0.772058824	0.032585083	0.412162162	0.227941176
8	0.360970311	0.536036036	0.542279412	0.639029689	0.463963964	0.457720588
9	0	0.84009009	0.110294118	1	0.15990991	0.889705882
10	0.608254888	0.189189189	0.720588235	0.391745112	0.810810811	0.279411765
11	0.090152064	1	0.439338235	0.909847936	0	0.560661765
12	0.234793628	0.189189189	0.417279412	0.765206372	0.810810811	0.582720588
13	0.769188993	0.849099099	0.884191176	0.230811007	0.150900901	0.115808824
14	0.349203476	0.486486486	0.514705882	0.650796524	0.513513514	0.485294118
15	0.353186097	0.587837838	0	0.646813903	0.412162162	1

Table 7. Grey relational co-efficient and grade

Run order	Grey relational co-efficient			Grey relational grade	Rank
	DOP	BH	BW		
	(larger the better)	(larger the better)	(smaller, the better)		
1	0.354425984	0.430283096	0.43943993	1.224149	9
2	0.440969581	0.248120301	0.611610793	1.300701	7
3	0.270349323	0.306194098	0.322576008	0.899119	15
4	0.496583963	0.66442953	0.326685107	1.487699	6
5	1	0.28813026	1	2.28813	1
6	0.643170237	0.444646759	0.821526634	1.909344	4
7	0.912543243	0.444646759	0.5914602	1.94865	3
8	0.347282625	0.415635992	0.418930272	1.181849	11
9	0.253731343	0.673593233	0.270557029	1.197882	10
10	0.464642666	0.289267946	0.541505792	1.295416	8
11	0.272033093	1	0.370511021	1.642544	5
12	0.307634853	0.289267946	0.361556433	0.958459	14
13	0.595643735	0.686212064	0.74022761	2.022083	2
14	0.343158249	0.391220763	0.404761905	1.139141	12
15	0.34454318	0.444646759	0.248120301	1.03731	13

Table 8. Experimental results

Trial	Voltage (V)	Travel Speed (mm/s)	% of CO_2 into the gas mixture	DOP (mm)	BH (mm)	BW (mm)
1	26	6	5	1.3568	5.024	6.878
2	26	6	5	1.2567	4.864	7.163
3	26	6	5	1.4342	5.132	6.998

GRA is utilized to determine the optimal condition of different input parameters to achieve the best characteristics or responses. GRA can be utilized to obtain the optimum conditions for multi-objective problems by providing weightage to individual responses. GRA is applied to evaluate the performance of a project with lesser/incomplete information. The steps involved in GRA are:

1. Normalization of data,
2. Calculation of deviation sequence, and
3. Determining grey relational coefficient.

Normalization of data is the pre-processing of raw data or original sequences into quantitative indices ranging from 0.00 to 1. The normalization of the original sequence or raw data is made according to the expected data sequence, either in the form of "higher-the-better" or "smaller-the-better". The deviation sequence ($\Delta oi(k)$) represents the absolute difference among the highest normalized values for each response. This Δoi (k) is used to calculate the grey relational coefficient, that indicates the relationship between the ideal and actual normalized experimental results.

The grey relation coefficient measures how well an experiment performs under different settings. The grey relational grade is defined as an average of grey relational coefficients of each response variable. The grey relational grade is important as it presents the strength of the relationship between two sequences. The higher grey relational grade is observed when the corresponding parameter combination is closer to the optimal.

The normalization and deviation sequence for responses (DOP, BH, and BW) is depicted in Table 7 The grey relational coefficient and grade for responses (DOP, BH, and BW) are depicted in Table 8. The weightage for DOP, BH, and BW was taken at 0.34, 0.33, and 0.33 to calculate the grey relational coefficient.

A higher grey relational grade was observed for run order 5, indicating that the corresponding combination of parameters is closer to optimal. The optimum value of the input variable for run order 5 was voltage = 26 V, travel speed = 6 mm/s, and 5% of CO_2 in the gas mixture.

Fig. 10 multilayer structure obtained with optimized parameters

An amalgamation of surface response practices and grey relational analyses is being used to convert multi-criteria optimization problems into a mono-corresponding objective function [25]. For the optimum input parameters (voltage = 26 V, travel speed = 6 mm/s, and 5% of CO_2 into gas mixture) obtained from the grey relation analysis, the experimental work was conducted in three sets. The outcomes of the experimental set are presented in Table 9. An average discrepancy in the result of experimentation was found to be less than 6%. The multilayer structure obtained from experimentation with the optimum parameter is presented in Figure 10**,** and the structure was found free from disbanding.

6. Conclusion

The prime aim of the present investigation was to optimize the input/process variables to obtain the optimum performance of the GMAW-based WAAM process using Metalloy 80B2 (1.00-1.50% chromium and 0.50% molybdenum steel), a gas-shielded metal-cored wire. The impact of variation in voltage (22 to 26 V), travel speed (1 to 6 mm/s), and shielding gas composition (CO_2 - 1%, 5%, and 9% and Argon - 99%. 95%, and 91%) was investigated on DOP, BH, and BW of bead deposition created using GMAW technique of WAAM. Metalloy 80B2, a gas-shielded metal-cored wire, was employed for bead deposition in single or multiple passes. The BBDs of RSM were used to obtain the optimum combination of input variables (voltage, travel speed, % of CO_2 into gas mixture) using Minitab v21 software for the experimental work. The GRA was conducted to obtain the optimal condition of input parameters to achieve the best response or characteristics.

For the outcomes of experimentation, the correlation for DOP, BH, and BW was developed as a function of input parameters such as % of CO_2 in a gas mixture, travel speed, and voltage. The significance of the model/ correlation was verified using ANOVA. The results of ANOVA indicated that travel speed was a more important parameter for the DOP and BH, whereas voltage is a more important parameter for BH. The p-value and F-value for lack of fit value obtained using ANOVA indicated that predicted correlations were adequate.

The main effect plot for the DOP, BH, and BW was studied to identify the most significant independent variable influencing the response. An increasing trend in DOP was observed with an increase in voltage, a decrease in travel speed, and an increase in % of CO_2 in the gas mixture. An increasing trend in BH was observed with an increase in voltage, an increase in travel speed, and an increase in % of CO_2 in the gas mixture. An increasing trend in BW was observed with a decrease in voltage, increase in travel speed, and increase in % of CO_2 in the gas mixture. The residual plots for DOP, BH, and BW were studied to assess the quality of developed correlations for DOP, BH, and BW. The error terms are closer to the straight line in the normal probability

plot of residuals for DOP, BH, and BW, indicating that error terms are normally distributed. The residuals are randomly distributed around the zero line in the residual versus fit plot for DOP, BH, and BW, indicating that the regression model is suitable for data sets. Asymmetric bell shape was not observed around zero in the histogram of a residual plot for DOP, BH, and BW, indicating a skewed distribution. The residuals fall randomly around the center line in the residual versus order plot for DOP, BH, and BW, indicating residuals are independent of one another. The GRA was studied to obtain the optimal condition of input variables (voltage, travel speed, and % of CO_2 in gas mixture) to obtain the best response. Using the GRA, the optimum value of input variables was obtained: voltage = 26 V, travel speed = 6 mm/s, and 5% of CO_2 in the gas mixture. For the optimum input parameters obtained from GRA, the experimental work was conducted, and an average discrepancy in the result of experimentation was found to be less than 6%. The multilayer structure obtained from experimentation with the optimum parameter was free from disbanding.

References

[1] Mohsen Attaran, "The Rise of 3-D Printing: The advantages of Additive Manufacturing Over Traditional Manufacturing," *Business Horizons*, vol. 60, no. 5, pp. 677-688, 2017. [CrossRef] [Google Scholar] [Publisher Link]

[2] Nor Ana Rosli et al., "Review on Effect of Heat Input for Wire Arc Additive Manufacturing Process," *Journal of Materials Research and Technology*, vol. 11, pp. 2127-2145, 2021. [CrossRef] [Google Scholar] [Publisher Link]

[3] Ilbey Karakurt, and Liwei Lin, "3D Printing Technologies: Techniques, Materials, and Post-Processing," *Current Opinion in Chemical Engineering*, vol. 28, pp. 134-143, 2020. [CrossRef] [Google Scholar] [Publisher Link]

[4] Vishal Kumar, Deepti Ranjan Sahu, and Amitava Mandal, "Parametric Study and Optimization of GMAW Based AM Process for Multi-Layer Bead Deposition," *Materials Today: Proceedings*, vol. 62, no. 1, pp. 255-261, 2022. [CrossRef] [Google Scholar] [Publisher Link]

[5] Cleber Marques et al., "Analysis of the Solid Wire Dip in the GMAW-CMT Melting Pool as a Means for Enhancing Additive Manufacturing," *Journal of the Brazilian Society of Mechanical Sciences and Engineering*, vol. 45, no. 3, 2023. [CrossRef] [Google Scholar] [Publisher Link]

[6] Jayaprakash Sharma Panchagnula, and Suryakumar Simhambhatla, "Manufacture of Complex Thin-Walled Metallic Objects using Weld-Deposition Based Additive Manufacturing," *Robotics and Computer-Integrated Manufacturing*, vol. 49, pp. 194-203, 2018. [CrossRef] [Google Scholar] [Publisher Link]

[7] Junbiao Shi et al., "Effect of In-process Active Cooling on Forming Quality and Efficiency of Tandem GMAW–Based Additive Manufacturing," *The International Journal of Advanced Manufacturing Technology*, vol. 101, pp. 1349-1356, 2019. [CrossRef] [Google Scholar] [Publisher Link]

[8] Philipp Henckel et al., "In Situ Production of Titanium Aluminides during Wire Arc Additive Manufacturing with Hot-Wire Assisted GMAW Process," *Metals*, vol. 9, no. 5, pp. 1-13, 2019. [CrossRef] [Google Scholar] [Publisher Link]

[9] Philipp Henckel et al., "Reduction of Energy Input in Wire Arc Additive Manufacturing (WAAM) with Gas Metal Arc Welding (GMAW)," *Materials*, vol. 13, no. 11, pp. 1-18, 2020. [CrossRef] [Google Scholar] [Publisher Link]

[10] Ashish Kumar, and Kuntal Maji, "Selection of Process Parameters for Near-Net Shape Deposition in Wire Arc Additive Manufacturing by Genetic Algorithm," *Journal of Materials Engineering and Performance*, vol. 29, pp. 3334-3352, 2020. [CrossRef] [Google Scholar] [Publisher Link]

[11] C.H. Bharat Kumar, and V. Anandakrishnan, "Experimental Investigations on the Effect of Wire Arc Additive Manufacturing Process Parameters on the Layer Geometry of Inconel 825," *Materials Today: Proceedings*, vol. 21, no. 1, pp. 622-627, 2020. [CrossRef] [Google Scholar] [Publisher Link]

[12] Justin Baby, and Murugaiyan Amirthalingam, "Microstructural Development during Wire Arc Additive Manufacturing of Copper-Based Components," *Welding in the World*, vol. 64, no. 2, pp. 395-405, 2020. [CrossRef] [Google Scholar] [Publisher Link]

[13] Adam M. Pringle et al., "Open Source Arc Analyzer: Multi-Sensor Monitoring of Wire Arc Additive Manufacturing," *HardwareX*, vol. 8, pp. 1-23, 2020. [CrossRef] [Google Scholar] [Publisher Link]

[14] E. Aldalur, A. Suarez, and F. Veiga, "Metal Transfer Modes for Wire Arc Additive Manufacturing Al-Mg alloys: Influence of Heat Input in Microstructure and Porosity," *Journal of Materials Processing Technology*, vol. 297, 2021. [CrossRef] [Google Scholar] [Publisher Link]

[15] Wenyong Zhao et al., "Modeling and Simulation of Heat Transfer, Fluid Flow and Geometry Morphology in GMAW-Based Wire Arc Additive Manufacturing," *Welding in the World*, vol. 65, no. 8, pp. 1571-1590, 2021. [CrossRef] [Google Scholar] [Publisher Link]

[16] Rama Kishore Mookara et al., "Influence of Droplet Transfer Behaviour on the Microstructure, Mechanical Properties and Corrosion Resistance of Wire Arc Additively Manufactured Inconel (IN) 625 Components," *Welding in the World*, vol. 65, no. 4, pp. 573-588, 2021. [CrossRef] [Google Scholar] [Publisher Link]

[17] Reyazul Warsi, Kashif Hasan Kazmi, and Mukesh Chandra, "Mechanical Properties of Wire and Arc Additive Manufactured Component Deposited by a CNC Controlled GMAW," *Materials Today: Proceedings*, vol. 56, no. 5, pp. 2818-2825, 2022. [CrossRef] [Google Scholar] [Publisher Link]

[18] Vishal Kumar et al., "Parametric Study and Characterization of Wire Arc Additive Manufactured Steel Structures," *The International Journal of Advanced Manufacturing Technology*, vol. 115, no. 5-6, pp. 1723-1733, 2021. [CrossRef] [Google Scholar] [Publisher Link]

[19] Teresa Artaza et al., "Wire Arc Additive Manufacturing Ti6Al4V Aeronautical Parts using Plasma Arc Welding: Analysis of Heat-Treatment Processes in Different Atmospheres," *Journal of Materials Research and Technology*, vol. 9, no. 6, pp. 15454-15466, 2020. [CrossRef] [Google Scholar] [Publisher Link]

[20] M.J. Bermingham et al., "High Strength Heat-Treatable β-Titanium Alloy for Additive Manufacturing," *Materials Science and Engineering: A*, vol. 791, 2020. [CrossRef] [Google Scholar] [Publisher Link]

[21] Rui Fu et al., "Large-size Ultra-High Strength-Plasticity Aluminum Alloys Fabricated by Wire Arc Additive Manufacturing Via Added Nanoparticles," *Materials Science and Engineering: A*, vol. 864, 2023. [CrossRef] [Google Scholar] [Publisher Link]

[22] Maximilian Gierth et al., "Wire Arc Additive Manufacturing (WAAM) of Aluminum Alloy AlMg5Mn with Energy-Reduced Gas Metal Arc Welding (GMAW)," *Materials*, vol. 13, no. 12, pp. 1-22, 2020. [CrossRef] [Google Scholar] [Publisher Link]

[23] Angela Dean, Daniel Voss, and Danel Draguljic, *Response Surface Methodology*, Design and Analysis of Experiments, 2nd ed., Springer International Publishing, pp. 565-614, 2017. [CrossRef] [Google Scholar] [Publisher Link]

[24] Andre I. Khuri, and Siuli Mukhopadhyay, "Response Surface Methodology," *WIREs Computational Statistics*, vol. 2, no. 2, pp. 128-149, 2010. [CrossRef] [Google Scholar] [Publisher Link]

[25] Yiyo Kuo, Taho Yang, and Guan-Wei Huang, "The Use of Grey Relational Analysis in Solving Multiple Attribute Decision-Making Problems," *Computers & Industrial Engineering*, vol. 55, no. 1, pp. 80-93, 2008. [CrossRef] [Google Scholar] [Publisher Link]